



SIZING AND TOPOLOGICAL OPTIMIZATION OF A SCIENTIFIC SATELLITE

Fernanda M. N. Ravetti

Mário Kataoka Filho

Luciana Assis de Castro

Instituto Nacional de Pesquisas Espaciais – DMC/INPE

Av. dos Astronautas, 1758

12.227-010 São José dos Campos, SP – Brazil

e-mail: {fernanda, kataoka}@dem.inpe.br – phone: +55-12-345-6245

Creto Augusto Vidal

Universidade Federal do Ceará – DC/UFC

Campus do PICI, Bloco 910, 60455-760 Fortaleza, CE – Brazil

e-mail: cvidal@lia.ufc.br – phone: +55 85 287-1333

Abstract. *The French-Brazilian Micro Satellite (FBMS) is a scientific satellite, which will be piggyback launched by the launcher Ariane 5. Its most critical design constraints are: the lower bound of 40.0 Hz on the first natural frequency, in order to avoid coupling between the launcher's excitation modes and the natural vibration modes of the satellite; and the upper bound of 10.5 kg on the structural mass. The structure of the FBMS is composed of a cylindrical aluminum alloy adapter for connection with the launcher, and eight sandwich panels (each composed of three layers) that define its topology. In this paper, it is shown the importance of structural optimization and design sensitivity analysis in the redesign cycles of Space Structures, by presenting all the steps taken and the difficulties encountered when trying to maximize the first natural frequency from the low value of 18.78 Hz obtained with the first trial design, while maintaining the structural mass below the predefined upper bound. All the modal and sensitivity analyses as well as the optimization steps were performed using MSC/NASTRAN. The design variable space for the structural optimization steps was composed of the thicknesses of the faces and core of the sandwich panels.*

Key-words: *Structural optimization, Sensitivity analysis, Space structures*

1. INTRODUCTION

Structural optimization seeks to find a point in a given design space (a set of design variables) so that a certain functional (objective function) is minimized or maximized. Usually, a number of constraint functionals, which depend on the design variables of the problem, and a set of lateral constraints on those design variables are imposed, delimiting the so called feasible region where the solution lies. Although structural optimization, as a field of studies, is not new (Dantzig, 1948; Kuhn & Tucker, 1950; Olhoff & Taylor, 1993), only in the

1980's did it really start to be applied to complex structural systems (Sobieszczanski, 1982). This was possible thanks to the increase in computer power and to the advances in optimization methods such as the method of feasible directions developed in that decade by (Vanderplaats, 1984) and used extensively since then. The gradient of the functionals with respect to the design variables, needed in that method, were computed by finite difference which was very costly. Since then, advances in Design Sensitivity Analysis formulations (Haber *at al.*, 1993; Moore, 1994), that made the design gradient computations very efficient, helped further to disseminate the use of structural optimization in complex structures. Nowadays, many of the advances in both structural optimization techniques (Bendsoe, 1995; Haftka & Gurdal, 1996; Olhoff, *at al.*, 1993) and design sensitivity analysis are implemented and, therefore, available in commercial finite element analysis software such as MSC/NASTRAN (Moore, 1994; Reymond & Miller, 1994).

In this paper, it is shown the importance of structural optimization and design sensitivity analysis in the redesign cycles of the French-Brazilian Micro Satellite (FBMS). First, it is presented the problem definition and the challenge for the structural optimization study. Next, it is described the analysis strategy and the steps taken to solve the structural optimization problem. Finally, the results are discussed and some conclusions are drawn.

2. PROBLEM DEFINITION

FBMS is a low terrestrial orbit scientific satellite which will be launched by the launcher Ariane 5. Its payload consists of the equipment for the following scientific experiments:

- FIRE – “Flare Infrared Experiment” – will perform continuous measurements of solar flares from space;
- PDP – “Plasma Diagnosis Package” – consists of three different plasma diagnosis experiments, which will measure plasma parameters of the ionosphere;
- CBEMG – “Confined Boiling Experiment under Microgravity” – will allow for the study of nucleation, of nucleate boiling and of heat flux, under microgravity conditions, along four test sections, each confined between two aluminum flat plates;
- CPL – “Capillary Pumped Loop” – will test a small scale capillary pumped loop in order to assess its performance under microgravity conditions;
- FLUXRAD – “Fluxmeter/Radiometer” – will measure the heat flux exchanged between FBMS' faces directed towards the sun and those facing the cold space.

FBMS' structure is composed of a cylindrical aluminum alloy adapter for connection with the launcher, and eight sandwich panels (each composed of three layers) that define its topology (see “Fig. 1”). The two external layers (faces) of those panels are made of aluminum sheet, which is a much stiffer material than that of the inner layer (core), composed of a low-density aluminum honeycomb (see “Fig. 2”). This type of sandwich configuration presents a high bending stiffness and a reduced weight.

After defining FBMS' topology and the type of sandwich panel to be used, a number of design constraints was established in order to perform some preliminary analyses. As a result of these analyses, an initial configuration was reached that satisfied all the design constraints except the one associated with the structure's first natural frequency. This initial configuration had a structural mass of 10.5 kg (equal to the upper bound on structural mass) and the first natural frequency of only 18.8Hz (well below the minimum allowable of 40.0Hz). The reason for this frequency constraint is to avoid coupling between the launcher's excitation modes and the natural vibration modes of the satellite. These two constraints are the most critical and difficult to satisfy because it is very hard to increase the stiffness of the structure without a corresponding increase of structural mass. Therefore, the structural design challenge is to refine the first trial design so that none of the constraints are violated.

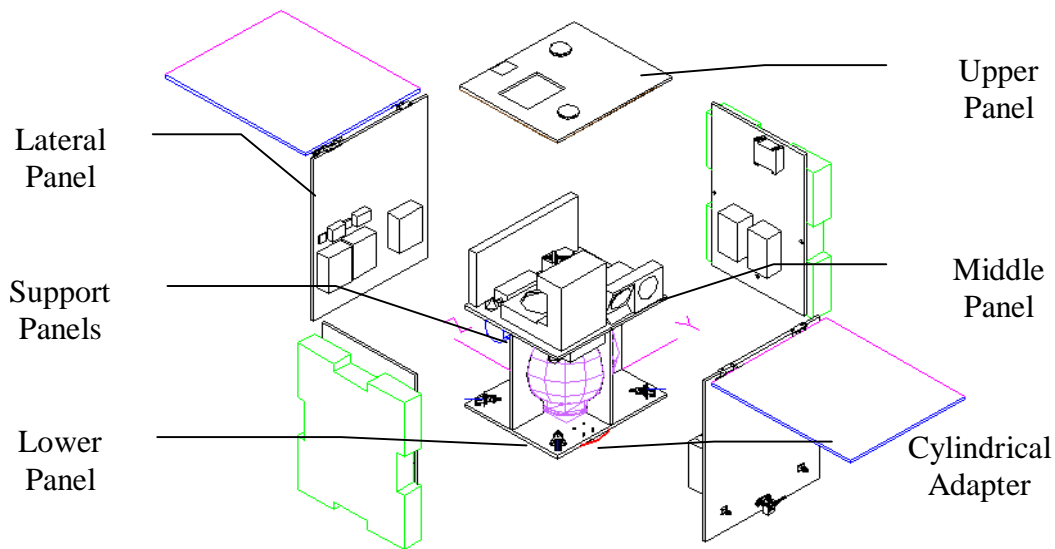


Figure 1 – Exploded view of the satellite

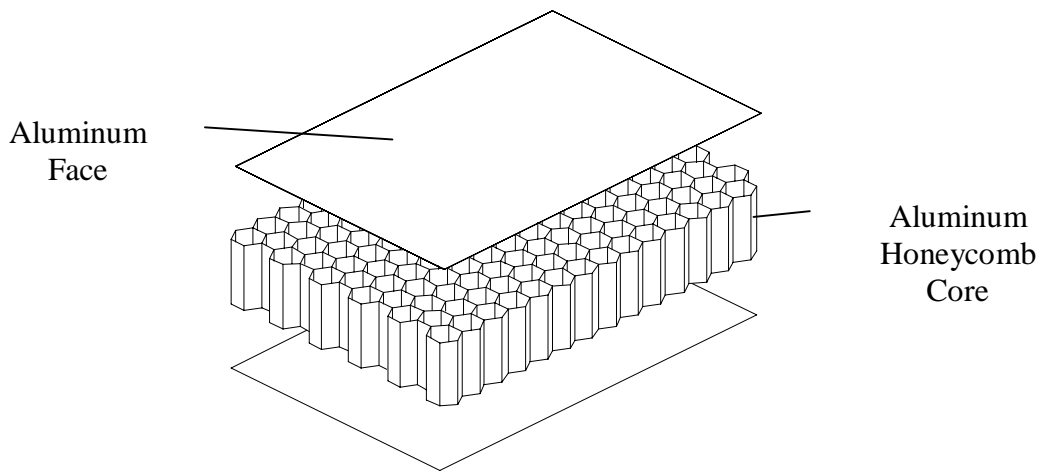


Figure 2 – Sandwich panel representation

In the next sections, it is discussed how structural optimization and design sensitivity analysis are used to find a feasible design of FBMS' structure.

3. ANALYSIS

3.1 The finite element model

The finite element model of the satellite was constructed using the pre- and post-processing package, (*FEMAP*, 1996). The cylindrical adapter was modeled by shell elements made of Aluminum 2024-T3, whose properties are defined in "Table 1." The eight sandwich panels were modeled by laminate shell elements which use the properties of Aluminum 2024-T3 for the faces and the properties of the aluminum honeycomb 3/8-5052-0.0015 for the core also listed in "Table 1." The total number of shell elements is 1,293, connected to a total of 1,114 nodes. The geometric properties of the shell elements are lumped in 9 different properties, one for each sandwich panel and one for the cylindrical adapter; the material properties are also lumped. The equipment loads were modeled as non-structural masses distributed over the panels. The spherical tank located at the center of the satellite is modeled

as a lumped mass, with translational and rotational inertia properties, positioned at its center of gravity. Interconnection of panels are modeled by rigid elements (NASTRAN's RBE2 element). Boundary conditions were simulated by single point constraints located at the attachment points of the cylindrical adapter to the launcher.

Before any stress or modal analysis was performed, a series of tests suggested by NASA (GIRD, 1994) to verify the correctness of the Finite Element model was done.

Table 1. Material properties

Material	Reference	Type	Young's modulus in N/m ²	Shear modulus in N/m ²	Poisson's ratio	Density in N/m ³
Aluminum	2024-T3	Isotropic	E = 6.80E+10	2.56E+10	0.33	2,700.00
Aluminum Honeycomb	3/8-5052-0.0015	Orthotropic	E ₁₂ = 1.000E+6		0.33	36.80
			E _{1z} = 2.206E+8			
			E _{2z} = 2.206E+8			

3.2 The optimization strategy

Here, the steps taken to maximize the FBMS' first natural frequency are described.

Step 1: Definition of the design space

A total of 16 design variables was defined: each face thickness (the faces of a panel have the same thickness) and each core thickness of the 8 sandwich panels.

Step 2: Preliminary optimization

Two preliminary optimizations, PO1 and PO2, were performed. The design variables' upper and lower bounds were arbitrarily set and a continuous variation was allowed.

$$\text{PO1: } \begin{cases} \text{Minimize } W \\ \text{subject to} \\ W \leq 10.5 \text{ kg} \\ \lambda_1 \geq 20\text{Hz} \\ 12.7 \times 10^{-5} \text{ m} \leq t_{\text{face}} \leq 1.0\text{m} \\ 1.0 \times 10^{-3} \text{ m} \leq t_{\text{core}} \leq 1.0\text{m} \end{cases}
 \quad
 \text{PO2: } \begin{cases} \text{Maximize } \lambda_1 \\ \text{subject to} \\ \lambda_1 \geq 20\text{Hz} \\ W \leq 10.5\text{kg} \\ 12.7 \times 10^{-5} \text{ m} \leq t_{\text{face}} \leq 1.0\text{m} \\ 1.0 \times 10^{-3} \text{ m} \leq t_{\text{core}} \leq 1.0\text{m} \end{cases}$$

where W is the structural weight, λ_1 is the first natural frequency in Hz, t_{face} are all the face thicknesses and t_{core} are all the core thicknesses.

Step 3: Preliminary optimization with commercial lower bound on t_{face}

This step is similar to Step 2, except that the lower bounds on the face thicknesses were set to the minimum aluminum plate thickness available in the market, 1.524E-4m. Notice that the honeycomb core is manufactured upon demand with the required thickness. We will refer to these optimization runs as POLB1 and POLB2.

Step 4: Optimization cycle with commercial thickness correction I

In this step, an optimization cycle based on POLB2 was performed, according to the following algorithm:

- i) Perform optimization POLB2 with the current set of design variables;
- ii) At the new location in the design space, look for the design variable which is closest to a commercial value;
- iii) Set the value of the design variable found in ii) to that commercial value and remove that variable from the design space;
- iv) Repeat i) to iii) until all the design variables are set to commercial values.

These optimization cycles will be referred to as OCI_i , where the index i ranges from one to the number of face thickness design variables.

Step 5: Design space reduction

In this step, a design sensitivity analysis was performed to identify the design variables which, when increased by a small amount, cause an increase in λ_1 (positive signs of the sensitivity array). In principle, these design variables should be eliminated from the design space (not allowed to vary) since they increase λ_1 at the expense of an increase in structural mass. In our case, the design variables corresponding to negative sensitivity terms have the most beneficial effect, since they increase λ_1 by means of structural mass reduction. One should exercise judgment when using sensitivity information to reduce the design space. Here, it is better not to eliminate a positive sensitivity design variable that has a strong effect on λ_1 , but only to allow little freedom for a mass increase which will be compensated by a mass reduction due to the negative sign sensitivity design variables. The design variables with close-to-zero sensitivity terms are eliminated from the design space and set to the lower bound.

Step 6: Optimization cycle with commercial thickness correction II

This cycle, referred to as $OCII_i$, is identical to OCI_i except that in step ii) we look for the design variables with smallest sensitivity terms.

Step 7: Changes in the lower panel

The design sensitivity analysis of Step 5 indicated that the design variables of the lower panel were the most effective in changing λ_1 , though through a mass increase. In this step, the optimized model of Step 6 was used as the basis for two new models that differ only on the composition of the lower panel. For the first model, seven types of honeycomb cores were tested ($HCLP_i$). The best of these models (model M1HC) was adopted as a base for the second model, which was completed by replacing the aluminum faces of the lower panel with a four-layer carbon fiber composite laminate. An optimization run was performed on model 2, here referred to as M2CF.

Step 8: Stiffening of the lower panel and adapter cylinder

Five new models were developed by placing stiffeners on either the lower panel, or on the adapter cylinder, or on both. New modal analyses were performed and the two models (MST1 and MST2) shown in “Fig. 3” were used for further optimization runs.



Figure 3 – Stiffened lower panels of models MST1 (left) and MST2 (right)

4. DISCUSSIONS

In this section, the results of each optimization strategy step are discussed.” The results of the preliminary optimizations PO1 and PO2 described in Step 2 are shown in “Table 2. PO1 presented a 35% reduction of the structural mass and a 6.4% increase in λ_1 , PO2 presented no reduction on the structural mass, but achieved a 10.2% increase in λ_1 .

Table 2. Results of preliminary optimizations PO1 and PO2

	$m_{\text{non-struct}}$ in kg	m_{struct} in kg	m_{total} in kg	λ_1 in Hz
Initial value	87.05	10.50	97.55	18.78
PO1	87.05	6.83	93.88	19.98
PO2	87.05	10.50	97.55	20.77

The results of the preliminary optimizations POLB1 and POLB2 described in Step 3 are displayed in “Table 3.” POLB1 presented a 33.6% reduction of the structural mass and a 6.5% increase in λ_1 , POLB2 presented no reduction on the structural mass and achieved a 14.4% increase in λ_1 .

Table 3. Results of preliminary optimizations POLB1 and POLB2

	$m_{\text{non-struct}}$ in kg	m_{struct} in kg	m_{total} in kg	λ_1 in Hz
Initial value	87.05	10.50	97.55	18.78
POLB1	87.05	6.97	94.02	20.00
POLB2	87.05	10.50	97.55	21.48

The results of the optimization cycles described by the algorithm of Step 4 (OCI) are displayed in “Table 4.” The column where it reads cycle 0 refers to the results of the preliminary optimization PO2 of Step2 and is displayed for comparison. The core thicknesses displayed in column 5 are rounded to millimeter. At the end of the eighth cycle, all the face thicknesses are set to commercial values and the optimum λ_1 is 22.83 Hz, which represents an increase of 21.6% relative to the first trial design and approximately 10% relative to the optimized value of PO2.

Table 4. Optimization cycle with commercial thickness correction - OCI

Cycles		0	1	2	3	4	5	6	7	8
Panels			Lat[+y]	Lat[+y]	Middle	Lower	Upper	Lat[-z]	Lat[+z]	Support
Design variables	Face	O	3.08e-4	3.01e-4	1.68e-4	1.56e-3	1.27e-4	2.45e-4	2.40e-4	1.27e-4
		C	3.05e-4	3.05e-4	1.52e-4	1.60e-3	1.52e-4	3.05e-4	3.05e-4	1.52e-4
	Core	O	1.50e-2	1.50e-2	1.54e-2	3.39e-2	1.50e-2	1.50e-2	5.00e-3	1.87e-2
		C	1.50e-2	1.50e-2	1.50e-2	3.40e-2	1.50e-2	1.50e-2	5.00e-3	1.90e-2
m_{total} (kg)		97.55	97.55	97.55	97.55	97.55	97.55	97.55	97.55	97.55
λ_1 (Hz)		20.77	20.72	22.31	22.93	22.85	22.80	22.67	22.78	22.83
Notes: Optimum (O) and Commercial (C) values of the design variables are in meters. Lat means lateral panel.										

The design sensitivity analysis of Step 5 computed the sensitivities of the first natural frequency of the satellite’s structure with respect to changes in the design variables. The results are presented in “Table 5.” Notice that, the larger the absolute value, the more sensitive the first natural frequency is to small changes in the corresponding design variable. For the FBMS, design sensitivity variables with negative sensitivity terms have a beneficial effect. However, the imposition of very tight lateral constraints on the design variables with positive sensitivities increases the first natural frequency at the expense of a modest increase

of mass. From the sensitivity values displayed, it is evident that the design variables associated with the Lower Panel are the most effective in increasing the first natural frequency. The sensitivity information is useful in reducing selectively the design space as was done in Step 6.

Table 5. Design sensitivity analysis of first natural frequency

Panel	Description	Sensitivities	
		w.r.t. face thickness	w.r.t. core thickness
1	Lower panel	7.1251 E+6	4.1293 E+5
2	Support panels	1.7865 E+6	2.4744 E+3
3	Middle panel	1.1914 E+6	4.7347 E+4
4	Lateral panel [-z]	4.7906 E+5	-2.0546 E+3
5	Lateral panel [+y]	1.6249 E+6	2.8084 E+4
6	Lateral panel [+z]	4.8121 E+5	-1.8696 E+3
7	Lateral panel [-y]	1.5855 E+6	2.5029 E+4
8	Upper panel	-7.5264 E+5	-4.2330 E+3

The results of the optimization cycles described in Step 6 (OCII) are displayed in “Table 6.” The line where it reads cycle 0 refers to the results of an optimization step where the eight design variables of the lateral panels were lumped in two design variables: the face thickness (considered the same for all the four panels) and the core thickness (also common to these panels). Notice that this was responsible for an increase of 30.2% in the frequency relative to the frequency of the first trial design. The core thicknesses displayed in column 5 are rounded to millimeter. The order of the cycles follow the order of elimination of the design variables with smaller sensitivity values from the design space. At the end of the fifth cycle, all the face thicknesses are set to commercial values and the optimum first natural frequency is 25.30 Hz, representing an increase of 34.7% relative to the first trial design.

Table 6. Optimization cycle with commercial thickness correction - OCII

Cycle	Panel	Design variable	Optimized value (m)	Commercial value (m)	Total mass (kg)	Frequency (Hz)
0					97.55	24.57
1	Upper	Face	1.27e-4	1.52e-4	97.55	23.37
		Core	1.50e-2	1.50e-2		
2	Middle	Face	1.27e-4	1.52e-4	97.55	25.65
		Core	1.57e-2	1.60e-2		
3	Lateral	Face	2.68e-4	3.05e-4	97.55	25.60
		Core	1.50e-2	1.50e-2		
4	Support	Face	1.94e-4	1.52e-4	97.55	25.57
		Core	2.50e-2	2.50e-2		
5	Lower	Face	1.34e-3	1.27e-3	97.42	25.30
		Core	5.0E-2	5.0E-2		

The properties of the honeycomb types used as the lower panel’s core material in the construction of the seven models M1HC described in Step 7 are displayed in “Table 7.” The results of the optimizations performed with each of the models are shown in “Table 8.” Notice that the best result was obtained with model M1HC7, which has the first natural frequency of

27.7 Hz. This represents an increase of 47.5% relative to the frequency of 18.78 Hz of the original model.

Table 7. Properties of honeycomb types for the Lower Panel of model M1HC

ID	HCLP1	HCLP2	HCLP3	HCLP4	HCLP5	HCLP6	HCLP7
Specification	3/8-5052-0.0015	1/4-5052-0.0040	1/4-5052-0.0020	1/4-5052-0.0015	1/4-5052-0.0010	3/8-5052-0.0025	3/8-5052-0.0040
Density(kg/m ³)	36.80	126.53	68.87	54.46	49.65	59.27	86.50
G _{1z} (MPa)	220.6	896.3	455.1	344.7	220.6	379.2	592.9
G _{2z} (MPa)	111.7	364.0	205.5	165.5	111.7	179.3	253.7

Table 8. Optimized frequencies for models M1HC's

Model ID	M1HC1	M1HC2	M1HC3	M1HC4	M1HC5	M1HC6	M1HC7
Honeycomb ID	HCLP1	HCLP2	HCLP3	HCLP4	HCLP5	HCLP6	HCLP7
Frequency in Hz	25.3	26.7	27.5	26.9	25.3	27.2	27.7

The faces of the lower panel of model M2CF (see Step7) are made of four-layer carbon fiber laminates with fibers arranged at 0°, 90°, 45° and -45° in each layer (the properties of carbon fibers are shown in “Table 9”). With this arrangement, the laminate has quasi-isotropic mechanical properties. The optimization step performed with this model considered as design variables only the thicknesses of the laminates' layers and the thickness of the honeycomb core of the lower panel. The results of this optimization are displayed in “Table 10,” where the results of model M1HC7 are also displayed for comparison. The first natural frequency was increased by approximately 6% relative to that of model M1HC7 which represents a total increase of 56.1% relative to λ_1 of the original model.

Table 9. Properties of Carbon Fibers

Property	Value
Material type	Orthotropic 2D
Modulus of elasticity in the longitudinal direction	200.0E+9N/m ²
Modulus of elasticity in the lateral direction	14.5E+9 N/m ²
Shear modulus	G ₁₂ = 4.9E+9 N/m ² G _{1z} = 4.9E+9 N/m ² G _{2z} = 4.9E+9 N/m ²
Poisson's ratio	v=0.3
Density	$\gamma=1650.N/m^3$

Table 10. Optimization results of models M1HC7 and M2CF

Description		m _{non-struct} (kg)	m _{struct} (kg)	m _{total} (kg)	λ_1
Model	M1HC7	87.05	10.50	97.55	27.70
	M2CF	87.05	10.50	97.55	29.32

The first natural frequencies of the stiffened models MST1 and MST2 prior and after optimization are displayed in “Table 11.” The frequency of 33.16Hz of the optimized MST2 model represents an increase of 76.6% relative to λ_1 of the original model.

Table 11. Optimization results of models MST1 and MST2

		Model	
		MST1	MST2
Frequency	Prior to optimization	30.88 Hz	32.32 Hz
	After optimization	32.11 Hz	33.16 Hz

5. CONCLUSIONS

The structure of the French-Brazilian Micro Satellite has two very critical design constraints: the lower bound of 40.0 Hz on the first natural frequency, in order to avoid coupling between the launcher's excitation modes and the natural vibration modes of the satellite; and the upper bound of 10.5 kg on the structural mass. This work demonstrates the importance of structural optimization and design sensitivity analysis in the redesign cycles of Space Structures, by presenting all the steps taken and the difficulties encountered in maximizing the first natural frequency from the low value of 18.78 Hz obtained with the first trial design, while maintaining the structural mass below the predefined upper bound. All the modal analyses, the sensitivity analyses and the optimization steps were performed using MSC/NASTRAN. The Method of Feasible Directions was used in all the optimization runs. The design variable space for the structural optimization steps was composed of the thicknesses of the faces and core of the sandwich panels.

After five optimization refinements on the initial model, the frequency was increased to 22.83 Hz, which represented an improvement of 21.6% relative to the initial design. The design sensitivity analysis helped to improve the model further, by making it possible to perform an optimization step with selective reduction of the design space, which resulted in a 34.7% increase of the first natural frequency relative to that of the first design. At that stage, still based on the sensitivity information, two new models were constructed: one, by changing the honeycomb properties of the lower panel's core; and the other, by using a different material (carbon fiber laminate) for the faces of the same panel. Two optimizations were performed with these models reaching a frequency of 29.32 Hz which corresponded to 56.1% improvement relative to the first natural frequency of the original model. By changing the topology of the satellite with the introduction of stiffeners attached to the lower panel and to the cylindrical adapter five models were constructed. The two best models were optimized and a first natural frequency of 33.16 Hz was achieved, representing a 76.6% increase relative to the first natural frequency of the original model.

From these studies, one concludes that Structural Optimization and Design Sensitivity Analysis are indispensable tools to the redesign process of Space Structures. In the case of the French Brazilian Micro Satellite, the first natural frequency increased 76.6% relative to its value at the beginning of the study, without any violation on its mass constraint. If structural optimization were not used, it would be impossible to achieve such a result without adding mass to the model. The design probably would be unfeasible, because of the high costs involved when excessive addition of mass occurs in space structures.

Despite the significant (76.6%) increase in the first natural frequency obtained through structural optimization and topology changes, the 113% improvement required to satisfy the lower bound constraint of 40 Hz on that frequency was not achieved. Nevertheless, this work demonstrates the important roles that structural optimization and design sensitivity analysis play in the redesign cycles of satellite structures.

Acknowledgments

The financial support of Conselho Nacional de Desenvolvimento Científico e Tecnológico (CNPq) and of Fundação de Amparo à Pesquisa do Estado de São Paulo (FAPESP) are gratefully acknowledged.

REFERENCES

- Bakhvalov, N., Panasenko, G., 1984, Homogenisation: Averaging, Processes in Periodic Media, Kluwer Academic Publishers, Dordrecht.
- Bendsoe, M. P., 1995, Optimization of Structural Topology, Shape, and Material, Springer-Verlag, Heidelberg.
- Dantzig, G. B., 1948, Programming in a Linear Structure, Comptroller, USAF, February, Washington, D. C..
- Haber, R.B., Tortorelli, D.A., Vidal, C.A. and Phelan, D.G., 1993, Design Sensitivity Analysis of Nonlinear Structures - I: Large-Deformation Hyperelasticity and History-Dependent Material Response, in Structural Optimization: Status & Promise, ed. M. P. Kamat, AIAA Progress in Astronautics and Aeronautics series, AIAA, New York, pp. 369-405,
- Haftka, Raphael, Gurdal, Zafer, 1996, Solid Mechanisms and its Application – Elements of Structural Optimization, Kluwer Academic Publishers, Dordrecht, The Netherlands.
- Kataoka, Mário Filho, 1997, Optimization of Nonhomogeneous Facesheets in Composite Sandwich Plates, Department of Aerospace Science and Engineering, University of Toronto, Toronto.
- Kuhn, H. W., Tucker, A. W., 1950, Nonlinear Programming, Proceedings of the 2d Berkeley Symposium on Mathematics, Statistics and Probability, Berkeley, California, pp. 481-492.
- Moore, Gregory J., 1994, User's Guide – MSC/Nastran – Design Sensitivity and Optimization, MSC – The MacNeal-Schwendler Corporation, Los Angeles.
- Olhoff, N., Thomsen, J., Rasmussen, J., 1993, Topology Optimization of Bi-Material Structures, in Optimal Design with Advanced Materials, ed. P. Pedersen, Elsevier Science Publisher B. V., Amsterdam, pp. 207-219.
- Olhoff, N., Taylor, J. E., 1993, On Structural Optimization, Journal of Applied Mechanics, vol. 50, Dec., pp. 1139-1151.
- Rao, J. R. J., Mistree, F., 1995, Recent Applications of Bilevel Models in Multidisciplinary Optimization, Proceedings of WCSMO-1: First World Congress of Structural and Multidisciplinary Optimization, eds. N. Olhoff and G. I. N. Rozvany, Pergamon, pp. 17-23.
- Reymond, Michael and Miller, Mark, 1994, MSC/NASTRAN – Quick Reference Guide, vers. 68, MSC – The MacNeal-Schwendler Corporation, Los Angeles.
- Sobieszcanski-Sobieski, J., 1982, A Linear Decomposition Method for Large Optimization Problems – Blueprint for Development, NASA TM 83248.
- Vanderplaats, Garret N., 1984, Numerical Optimization Techniques for Engineering Designs, Institute for Aerospace Studies, University of Toronto, Toronto.
- FEMAP, 1996, Introducing to FEA (Finite Element Analysis) using FEMAP (Finite Element Modeling and Postprocessing), Version 4.51 for Windows, Enterprise Software Products, Exton.
- GIRD, 1994, General Interface Requirements Document for EOS Common Spacecraft / Instruments, Goddard Space Flight Center, Greenbelt, Maryland, January.